Evidence for late Pleistocene volcanism at Santa Maria Island, Azores?

Ricardo S. Ramalho, Rui Quartau, Ármann Hóskuldsson, José Madeira, João Ventura da Cruz, Aurora Rodrigues

PII: S0377-0273(19)30562-1

DOI: https://doi.org/10.1016/j.jvolgeores.2020.106829

Reference: VOLGEO 106829

To appear in: *Journal of Volcanology and Geothermal Research*

Received date: 29 October 2019

Revised date: 18 February 2020

Accepted date: 25 February 2020

Please cite this article as: R.S. Ramalho, R. Quartau, Á. Hóskuldsson, et al., Evidence for late Pleistocene volcanism at Santa Maria Island, Azores?, *Journal of Volcanology and Geothermal Research*(2020), https://doi.org/10.1016/j.jvolgeores.2020.106829

Evidence for late Pleistocene volcanism at Santa Maria Island, Azores?

Ricardo S. Ramalho[a,b,c,d,*], Rui Quartau[e,a], Ármann Hóskuldsson[f], José Madeira[a,b], João Ventura da Cruz[e], Aurora Rodrigues[e]

[a] *Instituto Dom Luiz (IDL), Faculdade de Ciências, Universidade de Lisboa, 1749–016 Lisboa, Portugal*
[b] *Departamento de Geologia, Faculdade de Ciências, Universidade de Lisboa, 1749–016 Lisboa, Portugal*
[c] *School of Earth Sciences, University of Bristol, Wills Memorial Building, Queen's Road, Bristol, BS8 1RJ, UK*
[d] *Lamont-Doherty Earth Observatory at Columbia University, Comer Geochemistry Building, 61 Route 9W / PO Box 1000, Palisades, NY–10964–8000, USA*
[e] *Instituto Hidrográfico, Rua das Trinas 49, 1249–093 Lisboa, Portugal*
[f] *Nordvulk, Institute of Earth Sciences, University of Iceland, Sturlugata 7, 101 Reykjavk, Iceland*

Abstract

Santa Maria Island constitutes the oldest volcanic island within the Azores Archipelago, with no onshore record of eruptions younger than ≈ 2.8 Ma. A recent high-resolution multibeam bathymetric survey, however, revealed the presence of a seemingly young submerged wide volcanic edifice at approximately -70/-80 m, on the northeastern sector of the island shelf. The outer flanks of this volcanic edifice are partially eroded by marine erosion, but its general morphology is largely preserved, attesting to its relative youth. The edifice's aspect ratio and crater size are typical of a tuff ring formed by very violent surtseyan to taalian eruptions (with water/magma interaction ratios close to 1), implying extrusion at sea level or in very shallow waters, conditions that are incompatible with the present-day water depth at which this structure occurs. A detailed geomorphological analysis – coupled with a correlation with a modified

---

[*] Corresponding author. Tel.: +351 217 500 357

Email address: `raramalho@fc.ul.pt` (Ricardo S. Ramalho)

reference eustatic curve – allowed the formulation and discussion of a formation model for the tuff ring, which involves extrusion during a period immediately preceding a rapid relative sea-level drop, most likely at ≈ 43 ka. Extrusion during such a period would have allowed for the subaerial consolidation and palagonitization of the tuff ring, increasing its resistance to erosion, before being finally submerged during the Last Glacial Termination. Submersion during the Last Glacial Termination – a period characterised by extremely fast sea-level rise – also helps to explain why this tuff ring was submerged without being completely razed by marine erosion. Our study offers insights on the formation and preservation of tuff rings in coastal environments, and in relation to sea-level oscillations, suggesting that consolidation plays a crucial role in the process. Crucially, our study suggests that Santa Maria's volcanism might have extended well into the very late Pleistocene, raising important hazard implications. Future work is scheduled to confirm this hypothesis, including sampling of the volcanic products by dredging and/or by remote operated vehicle. Our study also emphasises the importance of available high-resolution bathymetric surveys to the formulation of solid volcanic hazard assessments on volcanic islands.

Keywords: recent volcanism, tuff ring, Azores, Santa Maria Island, multibeam bathymetry

1. Introduction

Volcanic hazard assessments simultaneously rely on knowledge of the present state of rest/unrest of an individual volcano and its past eruptive history (Sparks, 2003). Whilst the present state of a volcano – i.e. its current behaviour within the context of what is defined as its background or baseline behaviour – will inform us on the eventual probability of an eruption to take place in the near future, it is through the detailed analysis of that volcano's eruptive history that we gain knowledge on what type of eruptions are likely to occur, as well as on their expected characteristics and magnitude (Martí et al., 2008; Becerril et al., 2014, 2017). Also crucially, for long-term analysis, the detailed geological reconstruction of past eruptions and their age is key to estimate recurrence times between eruptions, and consequently to establish the greater or smaller likelihood for that volcano to erupt in a particular time frame (Newhall and Hoblitt, 2002; Sparks, 2003). Great importance is therefore given to information on when a particular volcano erupted for the last time, information that, when combined with estimates on recurrence time, will serve as the basis for the classification of that volcano as "active", "inactive", or "dormant" (Szakács, 1994).

At ocean island volcanoes, it is normally the age of the latest subaerial volcanism and/or the age of the latest noticeable shallow-water submarine volcanism (i.e. submarine volcanism that was either recorded during historical times or that left a recognisable imprint onshore) that is normally considered for volcanic hazard assessment purposes (Becerril et al., 2014, 2017). The subaerial portion of ocean island volcanoes, however, represents only a tiny fraction of the full geological record, which encompasses the shelf and submarine flanks of the island edifices. Given that high-quality marine geophysical and geological data on the submarine flanks of ocean islands are rarely available, it is therefore expected that many volcanic hazard assessments for ocean islands may be based on an incomplete record, consequently being subjected to an additional source of uncertainty (Becerril et al., 2013; Quartau et al., 2015a,b; León et al., 2017; Casalbore et al., 2018).

Here we report how a recent marine geophysical survey covering the shelf of Santa Maria – the oldest island in the Azores and a volcanic edifice considered extinct since the late Pliocene – will probably force us to reconsider the age of the latest eruptions on this island and, consequently, how we view potential volcanic hazard in the area. This survey employed high-resolution multibeam bathymetry and reflection seismic techniques to map the island shelf and its sedimentary cover. However, it unexpectedly revealed the presence of a seemingly young submerged wide cone (or tuff ring) on the northeastern sector of the island shelf, raising the possibility for volcanism to have extended well beyond 2.8 Ma, until recent times. In this letter we document the finding of this volcanic edifice and, using its morphology, discuss how and when it might have formed, an hypothesis to be tested by direct sampling during a future study. We also explore the possible implications arising from this discovery, namely to the perception of future volcanic hazard assessments on other ocean island volcanoes for which high-resolution marine geophysics is not available.

Figure 1: (a) Map illustrating the bathymetry and geotectonic setting of Santa Maria within the Azores triple junction. White arrows represent the approximate spreading direction of Terceira Rift (TR). Upper-right inset depicts the regional setting of the Azores archipelago within the North American (NA), Eurasian (Eu), and Nubian (Nu) triple junction, and the Mid-Atlantic Ridge (MAR). (b) Bathymetry/altimetry of Santa Maria Island edifice, prior to the recent high-resolution bathymetric survey. Bathymetry on both subfigures was extracted from the EMODNET web portal (http://portal.emodnet-bathymetry.eu); subaerial topography was generated from a 1:5000 scale digital altimetric database from Secretaria Regional do Turismo e Transportes of the Azores Government. (c) Shaded relief map of the subaerial part of Santa Maria Island (1:5000 scale, digital altimetric database) and surrounding shelf, the latter derived from the recent high-resolution multibeam bathymetric survey (see Ricchi et al., 2018). (d) Detailed high-resolution bathymetry of the inset in Fig. 1c, showing the seemingly young volcanic edifice (tuff ring) that constitutes de focus of this study and its surrounding submarine reliefs.

2. Geological setting

The Azores Archipelago is a group of nine volcanic islands located in the mid North Atlantic, in between $36.9° - 39.7°$ North latitudes and $24.7° - 31.5°$ West longitudes (Fig. 1a). The islands straddle the triple junction between the Eurasian, North American, and Nubian tectonic plates, and rest on the Azores Plateau, a large region of raised seafloor roughly defined by the -2000 m isobath (Needham and Francheteau, 1974; Louren¸ co et al., 1998; Gente et al., 2003; Miranda et al., 2018). With the exception of the westernmost islands of Flores and Corvo, which are located west of the Mid-Atlantic Ridge, all islands sit on the diffuse plate boundary between the Eurasian and Nubian plates, an area subjected to right-lateral transtensional strain that promoted magma ascent to the surface and contributed to the formation of these island edifices (Madeira and Ribeiro, 1990; Marques et al., 2013; Hipólito et al., 2013; Madeira et al., 2015; Miranda et al., 2015; Zanon, 2015; Miranda et al., 2018). Thus, on account of their geotectonic context, most of the Azores Islands are tectonically and volcanically active, with five islands exhibiting historical volcanism (i.e. since their discovery in the mid-15th century) and other two exhibiting holocene volcanism (Gaspar et al., 2015). Corvo Island had its last eruption at 80-100 ka (França et al., 2003), making Santa Maria the only island without evidence for recent onshore volcanism.

Having emerged for the first time above sea level at ≈ 6 Ma, Santa Maria is the oldest island in the Azores Archipelago (Ramalho et al., 2017). Its geological history comprises periods of intense volcanic growth (e.g. at 6.0–5.3 Ma, and at 4.1–3.5 Ma) alternated with periods of relative quiescence, during which erosion prevailed (Sibrant et al., 2015; Ramalho et al., 2017). At around 3.5 Ma, volcanism started to wane and island growth ceased, and at the same time the subsidence trend affecting the island edifice reversed to a slow uplift trend extending to recent times (Ramalho et al., 2017). The island's most recent period of volcanic activity recorded onshore comprises a set of monogenetic strombolian and hydromagmatic cones and associated pyroclastic deposits and lava flows of pliocene age (Serralheiro et al., 1987; Serralheiro, 2003; Ramalho et al., 2017). The products of this geological formation – representing low volume, sporadic volcanism – have been dated between 3.2 and 2.8 Ma, after which it is widely accepted that no volcanism occurred at Santa Maria (Sibrant et al., 2015; Ramalho et al., 2017). For this reason, volcanism at Santa Maria is regarded as extinct – and consequently volcanic hazard potential considered as very low – a condition that seems to be corroborated by the very low seismic activity recorded in the area (Gaspar et al., 2015; Fontiela et al., 2018).

Practically all studies on the evolution of Santa Maria Island and its volcanism relied exclusively on the island's onshore geological record, given that only low- to medium-resolution bathymetric datasets covering the island flanks and shelf were available until recently (see Fig. 1b). Therefore, notwithstanding the detailed knowledge of Santa Maria's onshore stratigraphy, until very recently little was known about the submarine flanks of the island, and how the geology of the offshore fitted in the already complex geological evolution model derived from subaerially-exposed sequences. A recent high-resolution bathymetric and seismic survey of Santa Maria's shelf and upper flanks, however, came to change this paradigm. This survey, which was conducted to characterise in detail the shelf and its sedimentary cover for marine aggregates and habitat mapping purposes, enabled a detailed mapping of the morphologies and geological structures located above the 200 m isobath, providing unique insights into the offshore geological record of Santa Maria (see Ricchi et al., 2018). Effectively, this new survey allowed the recognition of several morphologies – such as submerged marine terraces, fault scarps (many of which are the offshore extension of tectonic features recognised on land), sediment deposition traps, as well as volcanic structures (such as truncated cones and dykes exposed by marine erosion) – which are key to our stepwise comprehension of this island's evolutionary history (Ricchi et al., 2018, 2020). It was also during the course of this survey that the submerged volcanic edifice that constitutes the focus of this study was identified and mapped, leading to the preliminary results here reported.

3. Materials and Methods

A marine geophysical survey was undertaken onboard the R/V Arquipélago, from 24th August to 15th September 2016, in the scope of the FCT-funded project PLATMAR (*Development of volcanic island shelves: insights from Sta. Maria Island and implications on hazard assessment, habitat mapping and marine aggregates management*). The primary aim of this survey was to acquire new acoustic data (high-resolution multibeam bathymetry and single channel seismic reflection data) to better understand the evolution of Santa Maria's Island shelf and the dynamics of its sediment cover (Ricchi et al., 2018, 2020). Accordingly, high-resolution multibeam bathymetry was obtained using a pole-mounted Kongsberg EM2040C™ system with an operating frequency range of 200–400 KHz and angular coverage of 130°. The vessel position relied on DGPS with OMNISTAR corrections and survey track lines were generally run parallel to the isobaths and with an overlap to guarantee full seafloor coverage. Sound speed profiles were made during the survey using an AML MinosX Sound Velocity Profiler™ (SVP) to correct variations in sound velocity resulting from salinity and temperature changes along the water column. The survey comprised approximately 1330 multibeam lines, covering an area of c. 135 km^2, in between -20 m and -250 m. Bathymetric data was processed using the Caris software Hips & Sips 9.0 to produce high-resolution digital elevation models with variable cells size depending on water depth (1 m for shallow water to 8 m at c. -250 m). A dense network of 614 high-resolution seismic profiles was also acquired using an Applied Acoustic Engineering AA 200 Boomer™

plate, with most profiles using 100 J or 200 J of output energy, depending on the water depth. The receiver array consisted of a single channel streamer with 8 hydrophones. A total of 2008 km of seismic lines were acquired between -25 m and -300 m, made both parallel to the isobaths (and acquired concurrently with the multibeam survey) and perpendicular to the coastline, the latter with line spacing of ≈ 250 m.

The resulting high-resolution digital elevation model derived from the bathymetric mosaic was then analysed in a GIS environment, and morphologies mapped according to their typology. The eruptive edifice discussed in this study was then characterised with respect to its morphology, including measurements of its dimensions, aspect ratio, crater size vs overall diameter, the morphology of the flanks, etc. The two seismic lines that cross the edifice were then used to identify its internal structure (namely the geometry of its diatreme) and the thickness of the sedimentary cover. For relative sea-level correlations the eustatic curve of Bintanja and Van de Wal (2008) was used, and the uplift rates determined by Ramalho et al. (2017) and Ricchi et al. (2018) taken into account.

4. Results

4.1. Volcanic edifice location and setting

The volcanic edifice that constitutes the focus of this study is located on the northeast sector of Santa Maria’s insular shelf, at 37° 3’ 20.656” latitude North and 25° 4’ 52.073” longitude West (coordinates of its centre), and at approximately 75 m of water depth (see Fig. 1c and 1d). The edifice rests on a submerged marine terrace, extending over 1 km seawards from its inner edge, interpreted as a palaeo-shoreline presently located at -70/-80 m (see Fig. 7 of Ricchi et al., 2018). This terrace is interpreted to be polygenetic, formed and reworked by successive glacio-eustatic cycles over the last 0.8 Ma (Ricchi et al., 2018). The edifice is located approximately 350 m to the northeast of the said palaeo-shoreline, and is above a 2–3 m bathimetric step that can be seen immediately to its northeast.

Figure 2: Bathymetric profiles (a) across the volcanic edifice and their respective location (b), over detailed very high-resolution bathymetry of the area. Black arrows in (a) show inferred drowned wavecut notches and shoreline angle at the base of the ring. 3D views of the edifice from the southwest (c) and from the from the northeast (d) respectively; white arrows and black dashed line

point to inferred drowned wavecut notches and shoreangle at the base of the ring, respectively.

4.2. Bathymetric constraints on the edifice's dimensions and morphology

High-resolution bathymetry allowed us to constrain, very precisely, the present-day dimensions and morphology of the volcanic edifice. The edifice exhibits an elliptical shape, with 350 m and 250 m of longer and shorter axis, respectively, with the longer axis being oriented along the 315° azimuth. The crater is roughly circular, with 160 m in diameter. The rim stands approximately 6–8 m above the seafloor to the southwest of the edifice, and 10–12 m relatively to the seafloor on the deeper northeast side. The base of the edifice rises abruptly from the seafloor on all sides, and a clear morphological step can be seen practically all around the rim, both at its outer and inner slopes, at approximately -72 m (see bathymetric profiles of Fig. 2); this morphological step is, however, less evident on the north side, where the rim is lower. Lower arcuate relieves (with 1–2 m of elevation) are also observed concentrically arranged around the edifice's main relief, on its northwestern, northern, northeastern and eastern sides, and up to 100 m distant from the base of the edifice.

4.3. Reflection seismic constraints on the edifice's internal structure

Reflection seismic profiles (lines 3 and 57, Fig. 3) clearly show the internal structure of the edifice, with clear inward dipping reflectors inside the crater, interpreted as the diatreme of the vent. Sediment cover is also clearly seen in these profiles and amounts to 2-3 m in thickness, particularly inside the crater or on the landward side of the edifice (relatively to Santa Maria). The basal contact between the edifice and the underlying substrate cannot be seen in these profiles, due to technical limitations of the boomer system, which does not permit the detection of this contact.

Figure 3: Uninterpreted and interpreted seismic profiles (lines 3 and 57) across the volcanic edifice and their respective location. Note the presence of a well-developed diatreme below the edifice's crater, a structure typical of tuff cones/rings resulting from hydromagmatic eruptions.

5. Discussion

5.1. Morphological and structural constraints on eruption style and volcanic

edifice formation

Despite the fact that the outer flanks of the volcanic edifice are partially eroded, its general morphology is largely preserved, attesting to its relative young age. Moreover, the morphology and structure of the edifice can provide useful insights into the prevailing eruptive style and environmental conditions at the time of the eruption.

The edifice’s dimensions, aspect ratio, and crater size suggests it to be a very wide tuff cone or perhaps more accurately a tuff ring, morphologies that can be genetically linked to a monogenetic explosive hydromagmatic eruption (Cas and Wright, 1987; Schmincke, 2004). Effectively, notwithstanding the fact that it is partially eroded, the edifice exhibits a crater with small depth to width ratio at or above ground level and with a low rim, features that are typically associated with small but highly explosive hydromagmatic eruptions (Sheridan and Wohletz, 1981; Wohletz and Sheridan, 1983; Verwoerd and Chevallier, 1987; Sohn, 1996). In more detail, the edifice exhibits morphometric parameters that are typical for hydromagmatic tuff cones and tuff rings (see Pike, 1978). For example, on the basis of its actual dimensions, the edifice exhibits an average WCR/WCO (i.e. the ratio between the diameter of the crater and the diameter of the cone at its base) of 0.7, which is typical of tuff cones (Kervyn et al., 2012). However, if a wider, closer to the original diameter of the edifice prior to erosion (c. 450 m, as estimated from the seismic profiles of Fig. 3) is considered, this ratio lowers to 0.44, a value typical of tuff rings (Sheridan and Wohletz, 1981; Wohletz and Sheridan, 1983). Moreover, the edifice’s H/WCR (i.e. height/rim diameter ratio) is 0.07, which falls well within the typical range for tuff rings, i.e. between 0.13 and 0.05 (Pike, 1978; Wohletz and Sheridan, 1983; Vespermann and Schmincke, 2000). The reflection seismic profiles also show that the vent exhibits a well-developed diatreme, a defining characteristic of cones and rings formed by vigorous hydromagmatic eruptions (Lorenz and McBirney, 1970; Lorenz, 1986). Therefore, the morphology, dimensions, and structure of this volcanic edifice suggest it to be a tuff ring, formed by a violent surtseyan or more probably taalian eruption, implying water/magma ratios somewhere between ≈ 2 and ≈ 0.8 (e.g. see Wohletz and Sheridan, 1983). Such water/magma interaction ratios are generally attained when eruptive vents are located in very shallow waters or eventually onshore, on substrates with a near-surface saturated water table/body (Wohletz and Sheridan, 1983; Verwoerd and Chevallier, 1987; Sohn, 1996). In fact, similar structures in dimensions and morphology have been reported on the very shallow submerged coastal plains of Marion and Prince Edwards Islands in the Indian Ocean (see "type II" of Verwoerd and Chevallier, 1987); these rings exhibit characteristics that are intermediate between "wet" tuff cones and "dry" maar-type tuff rings, and are thought to have been formed during the Pleistocene and Holocene by drier, hotter and more violent explosions than those leading to the formation of tuff cones, although not as energetic as the preatomagmatic eruptions that generate tuff rings onshore (Verwoerd and Chevallier, 1987). Thus, by analogy, the characteristics of the studied volcanic edifice and surrounding plateau suggests that its genesis occurred on very shallow waters or even at sea level (e.g. see also Kano, 1998), i.e. during a period which relative sea level was necessarily 70–80 m lower than today's.

Modern examples of eruptions leading to the formation of coastal tuff cones and rings include the Capelinhos eruption on the western coast of Faial Island (Azores), which took place in 1957/58, the eruption of Surtsey (Iceland) in 1963–67, and more recently the eruption of Lake Vui (Ambae Island, Vanuatu) in 2005 and the eruption of Hunga Tonga-Hunga Ha to.666'apai (Tonga) in 2009 (Machado et al., 1962; Thorarinsson, 1966, 1967; Kokelaar, 1986; Németh et al., 2006; N´ emeth and Cronin, 2007; Vaughan and Webley, 2010). All of these eruptions occurred in relatively shallow waters, breached the sea/lake surface, and formed a tuff cone/ring above sea/lake level. Many of these examples, however, experienced a rapid change (from months to years) to a strombolian/hawaiian eruptive style once the vent was completely isolated from sea water, leading to late phase of subaerial cinder cone building or even the formation of a lava lake and lava flow shield. Given that the edifice reported here retained its ring-like morphology, without evolving to a taller tuff or cinder cone, it is postulated such a change to a strombolian/hawaiian eruptive style never happened, probably because this eruption was very short-lived and involved very low volumes of extruded material. Other examples of similar shallow-water-formed edifices that retained their ring-like morphology include Isla Tortuga in the Galápagos Islands and the islet of Molokini in Hawai to.666'i – see Fig. 4.

Figure 4: Subaerially exposed coastal tuff cones/rings that may serve as analogue for the submerged tuff ring offshore Santa Maria. (a) Isla Tortuga in the Galápagos Islands. (b) Ilhéu de Vila Franca (São Miguel, Azores). (c) and (d) Molokini, off Maui in Hawai to.666'i. Note the present-day wavecut notch marked by red arrows in (d). Images in (a), (b) and (d) correspond to Worldview Satellite Imagery accessed through Apple Maps™.

5.2. Erosional morphological imprint and inferred relative sea-level changes

The tuff ring rises abruptly from the seafloor on all sides suggesting that this structure has been partially eroded by marine erosion sometime after its formation, causing the reduction of its outer diameter and forming a small sea cliff. The lower concentric and outward-dipping relief that can be seen on the north and northeast sides of the ring is interpreted as the erosional remains of its outer flanks. The base of the ring therefore is thought to correspond the shore angle of a paleo shoreline at approximately -80 m, if we account for the 2-3 m thick present-day sedimentary cover that mantles the surroundings and abuts against the base of the edifice. The bathymetric step at -72 m is also interpreted as an incipient wavecut notch, carved at a higher position in the edifice. The presence of these two wavecut morphologies therefore attests to the positions of two distinct paleo sea levels, which timing will be here discussed. Crucially, the fact that these erosional morphologies are still preserved, implies that they were carved in an already largely consolidated tuff (which offered considerable resistance to wave cutting) given that the mechanical properties of weak and friable materials are not suitable for the preservation of steep coastal cliffs and notches (Trenhaile, 2015). The edifice also does not exhibit deep erosional gullies, slumps, or a significant topographical decay resulting from extended subaerial exposure.

The still largely preserved overall morphology of the ring implies that the ring was either exposed to marine erosion for only a very short period of time, i.e. not enough time elapsed to allow complete truncation by marine erosion pene-contemporaneous of the formation of the edifice (or during any of the subsequent sea levels that carved the wavecut features reported above), or particular conditions existed that allowed the ring to resist erosion. Crucially, considering its small size, it is highly unlikely such geological structure would survive largely intact if exposed to the abrasion of the surf zone during the passage of more than one glacio-eustatic cycle. Given these considerations, a correlation with a reference eustatic curve (e.g. Bintanja and Van de Wal, 2008) – modified to accommodate Santa Maria’s uplift rate determined by Ricchi et al. (2018) after Ramalho et al. (2017) – shows that there are only two, possibly three short time intervals for which the extrusion of the ring is likely (Fig. 5): (1) at 13.5–13.0 ka, the last period when sea level was at -80/-70 m; (2) at 54–43 ka, towards the end of a prolonged seastand during which sea level was fairly stationary at approximately -80 m, and before sea level dropped to the Last Glacial Maximum; or (3) eventually at 71.4–69.5 ka, the previous period that sea level was at -80/-70 m. Below we analyse each of these scenarios individually.

Figure 5: Eustatic curve by Bintanja and Van de Wal (2008) modified to accommodate Santa Maria's uplift rate of approximately 0.042 mm/yr reported by Ricchi et al. (2018). Note the 3 possible age intervals during which the eruption that gave rise to the tuff ring is inferred to have occurred. Age interval (2), 54–43 ka, is considered the most plausible, with eruption likely taking place closer to the lower age abound, i.e. at ≈ 43 ka. Subaerial exposure times (minimum and maximum) are indicated for extrusion at each age interval.

Extrusion followed by almost coeval rapid submergence at 13.5–13.0 ka is a plausible scenario (age interval 1 in Fig. 6). However, historical examples show that newly-formed, largely unconsolidated tuff cones/rings in the open ocean may be eroded away in a matter of months, years, or decades, particularly in highly-energetic seas such as that around the Azores (Ramalho et al., 2013). For example the tuff cone produced by the 1720 CE eruption of D. João de Castro Bank – which attained a diameter of 1.5 km and an elevation of about 250 m above sea level – was completely eroded to below sea level in two years (Agostinho, 1931; Weston, 1964). Similarly, the 90 m-high tuff cone produced by the Sabrina eruption (offshore Ponta da Ferraria in São Miguel) in 1811, was eroded in a matter of days (Madeira and Brum da Silveira, 2003). Syrtlingur, which formed during the eruption of Surtsey in 1963–67, was razed by marine erosion in just 7 days (Thorarinsson, 1966), presently being below -40 m (Romagnoli and Jakobsson, 2015). Even Capelinhos in Faial Island (Azores), which erupted in 1957/58 as the result of surtseyan and partly effusive eruption was reduced by coastal erosion to approximately 0.565 km^2 after just 50 years, and numerical modelling estimates that Capelinhos will be completely eroded in 100 years (Zhao et al., 2019). Coastal tuff cones and tuff rings are therefore, and in general, very ephemeral structures, unless special conditions exist to allow for their subaerial consolidation and higher resistance to wave action at a later stage (Hóskuldsson et al., 2007; Ramalho et al., 2013; Romagnoli and Jakobsson, 2015). We therefore suggest that the eruption and submergence of a tuff ring without significant erosion during a scenario of very rapid sea-level rise – even in one as rapid as the one that took place at 13.5–13.0 ka, during the Last Glacial Termination – is possible but unlikely.

More likely is a scenario where the eruption took place at sea level during a period of stable sea level and/or immediately preceding a period of rapid sea-level drop. This would allow for the subaerial consolidation of the tuff ring before surf was able to completely raze this structure. Post-eruptive consolidation through compaction and palagonitization of hydromagmatic tuffs, in a subaerial environment, may turn friable cones/rings into more stable and erosion-resistant structures (Jakobsson and Íslands, 1978; Jakobsson and Gudmundsson, 2008; Zanon et al., 2009). Palagonitization in particular constitutes the main mechanism for the consolidation of hydromagmatic and hyaloclastite tuffs. It consists in an alteration process that results from both rapid syn-eruptive hydrothermal activity or slower burial-diagenesis processes, and which gradually replaces sideromelane by hydrated gel-palagonite, palagonite, smectite and less commonly to zeolites (Jakobsson and Íslands, 1978; Jakobsson and Moore, 1986; Stroncik and Schmincke, 2001; Jakobsson and Gudmundsson, 2008; Pauly et al., 2011). Palagonitization as been reported to take place at very short time scales (i.e. a few years after eruption) but more commonly it takes place at the scale of a few thousands of years (Jakobsson and Gudmundsson, 2008; Zanon et al., 2009). As such, in our view it is more likely that the studied tuff ring was formed during the 54–43 ka seastand (age interval 2 in Fig. 5) when sea level was fairly stationary at approximately -80 m, before dropping to its minimum during the Last Glacial Maximum. Given that the ring does not show any obvious signs of significant topographical degradation due to prolonged subaerial erosion – and given that marine erosion pene-contemporaneous of the ring's formation was not able to completely raze its relief – it is more likely that its formation took place closer to 43 ka, immediately prior to the relative sea level drop of the Last Glacial Maximum rather than at an earlier stage. This would still result in 29.5–30.5 kyrs of subaerial exposure prior to submergence, a period that would possibly be long enough for the stabilisation, compaction and palagonitization of the ring but perhaps short enough to prevent excessive subaerial and marine erosion of this structure. Under this scenario, the carving of the lower wavecut surface, at the base of the ring, would be pene-contemporaneous of the ring's extrusion at ≈ 43 ka, whilst incipient marine erosion during submergence at 13.5–13.0 ka would have been responsible for the carving of the higher wavecut notch at -72 m. Accordingly, in our view, subaerial consolidation during the Last Glacial Maximum followed by rapid submergence of the ring during the very fast transgression of the Last Glacial Termination would explain why, albeit some erosion, the ring retained its young volcanic morphology and was not completely razed to the base.

Finally, the tuff ring could also have been formed at 71.4–69.5 ka (age interval 3 in Fig. 5), the previous time that sea level was at -80/-70 m. This scenario would be compatible with an extrusion at sea level or very shallow waters, and given that this period was characterised by a very rapid sea-level drop (by approximately 5.6 m/kyr), the tuff ring would be protected from marine erosion in just a few hundreds of years. Extrusion at 71.4–69.5 ka would also allow for subaerial consolidation over a period of approximately 57 ka, with some marine erosion of the base of the tuff ring taking place during the seastand at 54–43 ka, finally followed by rapid submergence and minor marine reworking (forming the higher wavecut notch) at approximately 13 ka. This scenario, however, would expose the ring to subaerial erosion for a considerably longer period, which presumably would result in a higher topographical degradation than the one inferred from the present-day morphology of the ring. We therefore consider that extrusion at ≈ 43 ka represents the more likely scenario.

5.3. Formation model

Given the aforementioned considerations, we propose that the tuff ring that is the focus of our study was formed at sea level or in very shallow waters by a violent surtseyan or more probably taalian eruption, which took place at a time when relative sea level was about 70 to 80 m lower than the present day's (see Fig. 6). This eruption resulted in the formation of a tuff ring about 20–30 meters high and 300–450 m of outer diameter. The eruption likely occurred at ≈ 43 ka, just before relative sea level dropped rapidly to its minimum at c. -122 m during the Last Glacial Maximum (20–18 ka). Extrusion at ≈ 43 ka would thus allow for the consolidation through compaction and palagonitization of the tuff ring, over a period of ≈ 30 ka, and allow only for weak marine erosion pene-contemporaneous of the extrusion of the ring. Subsequently, the tuff ring was rapidly submerged by the very fast transgression of the Last Glacial Termination, with only minor marine reworking, leaving it at the water depth it can be found today when sea level stabilised during the Holocene. In the meanwhile, shelf sediment deposition took place, covering the surroundings of the tuff ring with 2-3 m of sediment and partially infilling its crater.

Figure 6: Inferred formation model for the tuff ring, with modified eustatic curve on the right-hand side for reference. Stages correspond to: (1) Eruption of the tuff ring at sea level or in very shallow waters at ≈ 43 ka, when sea level was at 70–80 m below present level. (2) Incipient wave erosion of the base of the ring, pene-contemporaneous of the ring's formation. (3) Sea-level drop to -122 m

during the Last Glacial Maximum, allowing for the subaerial consolidation and palagonitization of the tuff ring, as well as some minor subaerial erosion. (4) Rapid sea-level rise during the Last Glacial Termination with further minor erosion of the base of the ring and the carving of wavecut notches at approximately at -72 m, during 13.5–13.0 ka. (5) Establishment of present-day sea level, leaving the tuff ring at its present water depth.

5.4. Implications & future work

The observations reported in this study, as well as the inferences on the probable age of the tuff ring and its relationship with sea-level oscillations, offer interesting insights into the processes of formation and preservation of coastal tuff rings and tuff cones. In particular we would like to stress what, in our view, is key to the preservation and survival of such morphologies beyond human time scales: the subaerial consolidation of tuffs through compaction and palagonitization prior to rapid marine erosion. Notwithstanding the fact that this inference is not anchored in direct observations of the ring's composition – our observations are restricted to the analysis of marine geophysical/acoustic data and does not include (yet) sampling of the tuff ring – the fundamental role of subaerial consolidation and rapid palagonitization in turning friable tuffs into erosion-resistant structures is well-documented by direct observations elsewhere (e.g. Jakobsson and Íslands, 1978; Jakobsson and Moore, 1986; Stroncik and Schmincke, 2001; Jakobsson and Gudmundsson, 2008; Pauly et al., 2011), and should be taken into account when studying submerged tuff rings such as this. Moreover, the considerations in this study suggest that consolidation/palagonitization of tuffs prior to rapid marine erosion is only possible if those tuff rings and tuff cones are formed at sea level or in very shallow waters (i.e. the bulk of its volume is above water) during – or immediately preceding – periods of very rapid relative sea-level drop, or alternatively had to experience very rapid syn-eruptive hydrothermal palagonitization to ensure their survival above sea level. This suggests that morphologically preserved tuff cones/rings such as Isla Tortuga (Galápagos Islands), Molokini (Hawai‘i), Ilhéu de Vila Franca (São Miguel, Azores), Ilhéus das Cabras (Terceira, Azores) – all of which are well-consolidated and highly-palagonitized – were probably extruded during or immediately preceding periods of rapid sea-level drop, generally at the end of interglacials, or alternatively were the subject of very rapid syn-eruptive palagonitization. Otherwise, as historical examples in the Azores and Iceland show, marine erosion rapidly obliterates such structures, particularly when they rise from deeper waters and are exposed to the open ocean (Quartau et al., 2014; Romagnoli and Jakobsson, 2015; Zhao et al., 2019). This hypothesis remains to be tested with isotopic geochronology, but nevertheless it highlights how crucial it is to integrate eruption timing with information on relative sea-level to better understand the formation and preservation of coastal/shallow water tuff rings and cones in relation to their environmental factors. Moreover, if a clear relationship between edifice morphology and position of the vent with respect to coeval sea-level is firmly established, we may be able to create a framework that we can use to more critically look at isotopic ages with large uncertainties, and narrow those uncertainties on the basis of higher likelihood of eruption in correlation to relative and eustatic curves.

Importantly, if our considerations are correct, volcanism at Santa Maria extended beyond the ≈ 2.8 Ma age threshold inferred from subaerially-exposed sequences, well into the late Pleistocene. This means that Santa Maria probably experienced low-volume and sporadic volcanism at least once in the last 100 ka, raising important hazard implications. Notwithstanding the uncertainty concerning the exact timing of eruption of this tuff ring, its presence suggests that volcanic hazard assessments for Santa Maria should take into account the occurrence of volcanic activity on this island during the last 100 ka, after a long period of volcanic quiescence. Crucially, this work also highlights how the availability of high-resolution marine geophysics/acoustic data for the flanks and shelf of ocean island volcanoes is key to a solid and more accurate formulation of volcanic hazard assessments. Solely based on onshore data, volcanic hazard assessments rely only on part of the geological record, preventing a cabal and complete view on the timing (and type) of the latest volcanic activity of the edifice, as well as an incomplete view concerning the frequency of eruptions, i.e. the recurrence time between eruptions in that particular volcanic edifice. This is particularly applicable to edifices subjected to recurrent dispersed and parasitic monogenetic volcanism in their flanks, as it happens during the rejuvenated stages of many islands, or in some contexts during any stage of island evolution (e.g. such as in the Azores).

Finally, future work is planned to recover samples from the studied tuff ring through dredging and/or sampling by remote operated vehicle. These samples will allow us to confirm the age and composition of this structure, as well as provide insights on the geochemistry of the youngest volcanic manifestation at Santa Maria, one whose existence would go unnoticed without the acquisition of high-resolution bathymetry in this island.

6. Conclusions

This study documents the existence of a seemingly young submerged tuff ring at Santa Maria island shelf, presently at 70–80 m of water depth. A detailed analysis of the morphology of the tuff ring and its internal structure suggests it to be a partially eroded tuff ring extruded by a hydromagmatic eruption that took place at sea level or in much shallower waters than the depth at which can be observed today. This analysis – coupled with a correlation with a modified reference eustatic curve – allowed the formulation and discussion of a formation model for the tuff ring, which involves extrusion just prior to a period of rapid relative sea-level drop, most likely at ≈ 43 ka. Extrusion during such a period would have allowed for the subaerial consolidation of the tuff ring, increasing its resistance to erosion, before being finally submerged during the Last Glacial Termination – a period characterised by extremely fast sea-level rise – explaining why the tuff ring was submerged without being completely razed by marine erosion. Our observations therefore suggest that Santa Maria's volcanic activity might have extended into the very late Pleistocene, raising important hazard implications. Future work is scheduled to confirm this hypothesis, including sampling of the volcanic products during a dedicated research cruise. Our study also highlights how the availability of high-resolution bathymetric surveys is crucial for more solid and realistic volcanic hazard assessments.

Acknowledgments:

This work was supported by the projects PTDC/GEO-GEO/0051/2014 PLATMAR, and UID/GEO/50019/2019 and UIDB/50019/2020 – Instituto Dom Luiz, all funded by Fundação para a Ciência e Tecnologia. R. Ramalho and R. Quartau would like to acknowledge their IF/01641/2015 and IF/00635/2015 Investigador FCT contracts. The authors thank J. Martí and an anonymous reviewer for their insightful comments that helped to improve this manuscript.

References

Agostinho, J., 1931. The volcanoes of the Azores Islands. Bulletin Volcanologique 8 (1), 123–138.

Becerril, L., Bartolini, S., Sobradelo, R., Martí, J., Morales, J., Galindo, I., 2014. Long-term volcanic hazard assessment on El Hierro (Canary Islands). Natural Hazards and Earth System Sciences 14 (7), 1853–1870.

Becerril, L., Cappello, A., Galindo, I., Neri, M., Del Negro, C., 2013. Spatial probability distribution of future volcanic eruptions at El Hierro Island (Canary Islands, Spain). Journal of volcanology and geothermal research 257, 21–30.

Becerril, L., Martí, J., Bartolini, S., Geyer, A., 2017. Assessing qualitative long-term volcanic hazards at Lanzarote Island (Canary Islands). Natural Hazards and Earth System Sciences 17 (7), 1145–1157.

Bintanja, R., Van de Wal, R., 2008. North American ice-sheet dynamics and the onset of 100,000-year glacial cycles. Nature 454 (7206), 869–872.

Cas, R., Wright, J., 1987. Volcanic Successions. Modern and Ancient: a Geological Approach to Processes, Products and Successions. Chapman & Hall, London, UK.

Casalbore, D., Romagnoli, C., Bosman, A., De Astis, G., Lucchi, F., Tranne, C., Chiocci, F., 2018. Multi-stage formation of La Fossa Caldera (Vulcano Island, Italy) from an integrated subaerial and submarine analysis. Marine Geophysical Research, 1–14.

Fontiela, J., Sousa Oliveira, C.., Rosset, P., 2018. Characterisation of Seismicity of the Azores Archipelago: An Overview of Historical Events and a Detailed Analysis for the Period 2000–2012. In: Kueppers, U., Beier, C. (Eds.), Volcanoes of the Azores. Active Volcanoes of the World. Springer, Berlin, Heidelberg.

França, Z., Nunes, J., Cruz, J., Duarte, H., Forjaz, V., Garcia, F., Valero, J. L., 2003. Estudo preliminar do vulcanismo da Ilha do Corvo, Açores. In: 727-730 (Ed.), Proceedings da 3a Assembleia Luso-Espanhola de Geodesia e Geofisica. Vol. 2. Univ. Politécnica de Valencia.

Gaspar, J. L., Queiroz, G., Ferreira, T., Medeiros, A. R., Goulart, C., Medeiros, J., 2015. Chapter 4 Earthquakes and volcanic eruptions in the Azores region: geodynamic implications from major historical events and instrumental seismicity. Geological Society, London, Memoirs 44 (1), 33–49.

Gente, P., Dyment, J., Maia, M., Goslin, J., 2003. Interaction between the Mid-Atlantic Ridge and the Azores hot spot during the last 85 Myr: Emplacement and rifting of the hot spot-derived plateaus. Geochemistry, Geophysics, Geosystems 4 (10), 8514.

Hipólito, A., Madeira, J., Carmo, R., Gaspar, J. L., 2013. Neotectonics of Graciosa Island (Azores): a contribution to seismic hazard assessment of a volcanic area in a complex geodynamic setting. Annals of Geophysics 56 (6).

Hóskuldsson, A., Hey, R., Kjartansson, E., Gudmundsson, G. B., 2007. The Reykjanes Ridge between 63° 10 N and Iceland. Journal of Geodynamics 43 (1), 73–86.

Jakobsson, S. P., Gudmundsson, M. T., 2008. Subglacial and intraglacial volcanic formations in Iceland. Jökull 58, 179–196.

Jakobsson, S. P., Íslands, N., 1978. Environmental factors controlling the palagonitization of the Surtsey tephra, Iceland. Museum of Natural History, Department of Geology and Geography.

Jakobsson, S. P., Moore, J. G., 1986. Hydrothermal minerals and alteration rates at Surtsey volcano, Iceland. Geological Society of America Bulletin 97 (5), 648–659.

Kano, K., 1998. A shallow-marine alkali-basalt tuff cone in the middle Miocene Jinzai formation, Izumo, SW Japan. Journal of Volcanology and Geothermal Research 87 (1), 173 – 191.

Kervyn, M., Ernst, G., Carracedo, J.-C., Jacobs, P., 2012. Geomorphometric variability of “monogenetic” volcanic cones: evidence from Mauna Kea, Lanzarote and experimental cones. Geomorphology 136 (1), 59–75.

Kokelaar, B., 1986. Magma-water interactions in subaqueous and emergent basaltic. Bulletin of Volcanology 48 (5), 275–289.

León, R., Somoza, L., Urgeles, R., Medialdea, T., Ferrer, M., Biain, A., García-Crespo, J., Mediato, J. F., Galindo, I., Yepes, J., et al., 2017. Multi-event oceanic island landslides: New onshore-offshore insights from El Hierro Island, Canary Archipelago. Marine Geology 393, 156–175.

Lorenz, V., 1986. On the growth of maars and diatremes and its relevance to the formation of tuff rings. Bulletin of volcanology 48 (5), 265–274.

Lorenz, V., McBirney, A.R.nand Williams, H., April 1970. An investigation of volcanic depressions. Part 3: Maars, tuff-rings, tuff-cones, and diatremes. Progress Report NASA Research Grant NGR-38-003-012, Center for Volcanology, University of Oregon, Eugene, Oregon.

Lourenço, N., Miranda, J., Luis, J., Ribeiro, A., Victor, L. M., Madeira, J., Needham, H., 1998. Morpho-tectonic analysis of the Azores Volcanic Plateau from a new bathymetric compilation of the area. Marine Geophysical Researches 20 (3), 141–156.

Machado, F., Parsons, W. H., Richards, A. F., Mulford, J. W., 1962. Capelinhos eruption of Fayal volcano, Azores, 1957–1958. Journal of Geophysical Research 67 (9), 3519–3529.

Madeira, J., Brum da Silveira, A., 2003. Active tectonics and first paleoseismological results in Faial, Pico and S. Jorge islands (Azores, Portugal). Annals of Geophysics 46 (5), 733–761.

Madeira, J., Brum da Silveira, A., Hipólito, A., Carmo, R., 2015. Chapter 3 Active tectonics in the central and eastern Azores islands along the Eurasia–Nubia boundary: a review. Geological Society, London, Memoirs 44 (1), 15–32.

URL `http://mem.lyellcollection.org/content/44/1/15`

Madeira, J., Ribeiro, A., 1990. Geodynamic models for the Azores triple junction: a contribution from tectonics. Tectonophysics 184 (3), 405–415.

Marques, F. O., Catalão, J. C., DeMets, C., Costa, A. C. G., Hildenbrand, A., 2013. GPS and tectonic evidence for a diffuse plate boundary at the Azores Triple Junction. Earth and Planetary Science Letters 381, 177–187.

Martí, J., Aspinall, W., Sobradelo, R., Felpeto, A., Geyer, A., Ortiz, R., Baxter, P., Cole, P., Pacheco, J., Blanco, M., Lopez, C., 2008. A long-term volcanic hazard event tree for Teide-Pico Viejo stratovolcanoes (Tenerife, Canary Islands). Journal of Volcanology and Geothermal Research 178 (3), 543 – 552, evaluating Explosive Eruption Risk at European Volcanoes.

Miranda, J. M., Luis, J. F., Lourenço, N., 2018. The Tectonic Evolution of the Azores Based on Magnetic Data. In: Kueppers, U., Beier, C. (Eds.), Volcanoes of the Azores. Active Volcanoes of the World. Springer, Berlin, Heidelberg.

Miranda, J. M., Luis, J. F., Lourenço, N., Fernandes, R. M. S., 2015. Chapter 2 The structure of the Azores Triple Junction: implications for São Miguel Island. Geological Society, London, Memoirs 44 (1), 5–13.

URL `http://mem.lyellcollection.org/content/44/1/5`

Needham, H., Francheteau, J., 1974. Some characteristics of the rift valley in the Atlantic Ocean near 36° 48' north. Earth and Planetary Science Letters 22 (1), 29–43.

Németh, K., Cronin, S., 2007. Syn- and post-eruptive erosion, gully formation, and morphological evolution of a tephra ring in tropical climate erupted in 1913 in West Ambrym, Vanuatu. Geomorphology 86 (1), 115 – 130.

URL `http://www.sciencedirect.com/science/article/pii/S0169555X06003862`

Németh, K., Cronin, S. J., Charley, D. T., Harrison, M. J., Garae, E., 2006. Exploding lakes in Vanuatu-" surtseyan-style" eruptions witnessed on Ambae Island. Episodes 2006 (29), 87–92.

Newhall, C., Hoblitt, R., Mar 2002. Constructing event trees for volcanic crises. Bulletin of Volcanology 64 (1), 3–20.
URL `https://doi.org/10.1007/s004450100173`

Pauly, B. D., Schiffman, P., Zierenberg, R. A., Clague, D. A., 2011. Environmental and chemical controls on palagonitization. Geochemistry, Geophysics, Geosystems 12, Q12017.

Pike, R. J., 1978. Volcanoes on the inner planets – Some preliminary comparisons of gross topography. In: Lunar and Planetary Science Conference Proceedings. Vol. 9. pp. 3239–3273.

Quartau, R., Hipólito, A., Mitchell, N., Gaspar, J., Brandão, F., 2015a. Comment on "Construction and destruction of a volcanic island developed inside an oceanic rift: Graciosa Island, Terceira Rift, Azores" by Sibrant et al.(2014) and proposal of a new model for Graciosa's geological evolution. Journal of Volcanology and Geothermal Research 303, 146–156.

Quartau, R., Hipólito, A., Romagnoli, C., Casalbore, D., Madeira, J., Tempera, F., Roque, C., Chiocci, F. L., 2014. The morphology of insular shelves as a key for understanding the geological evolution of volcanic islands: Insights from Terceira Island (Azores). Geochemistry, Geophysics, Geosystems 15 (5), 1801–1826.

Quartau, R., Madeira, J., Mitchell, N., Tempera, F., Silva, P., Brandão, F., 2015b. The insular shelves of the Faial-Pico Ridge: A morphological record of its geologic evolution (Azores archipelago). Geochem. Geophys. Geosyst 16, 1401–1420.

Ramalho, R. S., Helffrich, G., Madeira, J., Cosca, M., Thomas, C., Quartau, R., Hipólito, A., Rovere, A., Hearty, P. J., Ávila, S. P., October 2017. Emergence and evolution of Santa Maria Island (Azores) – The conundrum of uplifted islands revisited. Geological Society of America Bulletin 129 (3/4), 372–391.

Ramalho, R. S., Quartau, R., Trenhaile, A. S., Mitchell, N. C., Woodroffe, C. D., Ávila, S. P., 2013. Coastal evolution on volcanic oceanic islands: A complex interplay between volcanism, erosion, sedimentation, sea-level change and biogenic production. Earth-Science Reviews 127 (0), 140 – 170.

Ricchi, A., Quartau, R., Ramalho, R., Romagnoli, C., Casalbore, D., 2020. Imprints of volcanic, erosional, depositional, tectonic and mass-wasting processes in the morphology of Santa Maria insular shelf. Marine Geology in review.

Ricchi, A., Quartau, R., Ramalho, R. S., Romagnoli, C., Casalbore, D., da Cruz, J. V., Fradique, C., Vinhas, A., 2018. Marine terrace development on reefless volcanic islands: New insights from high-resolution marine geophysical data offshore Santa Maria Island (Azores Archipelago). Marine Geology 406, 42–56.

Romagnoli, C., Jakobsson, S., 2015. Post-eruptive morphological evolution of island volcanoes: Surtsey as a modern case study. Geomorphology 250, 384–396.

Schmincke, H.-U., 2004. Volcanism, 1st Edition. Springer Verlag, Berlin Heilderberg, Germany.

Serralheiro, A., 2003. A geologia da ilha de Santa Maria, Açores. Açoreana 10 (1), 141–192.

Serralheiro, A., Alves, C. A. M., Forjaz, V. H., Rodrigues, B., 1987. Carta Vulcanológica dos Açores. Ilha de Santa Maria na escala 1/15 000 (folhas 1 e 2). Tech. rep., Serviço Regional de Protecção Civil dos Açores, Universidade dos Açores and Centro de Vulcanologia.

Sheridan, M. F., Wohletz, K., 1981. Hydrovolcanic explosions: The systematics of water-pyroclast equilibration. Science 212 (4501), 1387–1389.
URL `https://science.sciencemag.org/content/212/4501/1387`

Sibrant, A. L. R., Hildenbrand, A., Marques, F. O., Costa, A. C. G., 2015. Volcano-tectonic evolution of the Santa Maria Island (Azores): Implications for paleostress evolution at the western Eurasia–Nubia plate boundary. Journal of Volcanology and Geothermal Research 291, 49–62.

Sohn, Y. K., 1996. Hydrovolcanic processes forming basaltic tuff rings and cones on Cheju Island, Korea. Geological Society of America Bulletin 108 (10), 1199–1211.

Sparks, R., 2003. Forecasting volcanic eruptions. Earth and Planetary Science Letters 210 (1), 1 – 15.

Stroncik, N. A., Schmincke, H.-U., 2001. Evolution of palagonite: Crystallization, chemical changes, and element budget. Geochemistry, Geophysics, Geosystems 2 (7).

Szakács, A., Nov 1994. Redefining active volcanoes: a discussion. Bulletin of Volcanology 56 (5), 321–325.

Trenhaile, A. S., 2015. Notches, Sea-level change, Wave erosion, Weathering, Bioerosion. Earth-Science Reviews 150, 285–304

Thorarinsson, S., 1966. Surtsey eruption course of events and development of the new island.

Surtsey Research Progress Report II, 117–123.

Thorarinsson, S., 1967. Surtsey: the new island in the North Atlantic. Viking Press.

Vaughan, R. G., Webley, P. W., 2010. Satellite observations of a surtseyan eruption: Hunga Ha'apai, Tonga. Journal of Volcanology and Geothermal Research 198 (1), 177 – 186. URL `http://www.sciencedirect.com/science/article/pii/S0377027310002635`

Verwoerd, W., Chevallier, L., 1987. Contrasting types of surtseyan tuff cones on Marion and Prince Edward islands, southwest Indian Ocean. Bulletin of Volcanology 49 (1), 399–413.

Vespermann, D., Schmincke, H., 2000. Scoria cones and tuff rings. In: Sigurdsson, H., Houghton, B., McNutt, S., Rymer, H., Stix, J. (Eds.), Encyclopedia of Volcanoes, 1st Edition. Academic Press, USA, pp. 683–694.

Weston, F., 1964. List of recorded volcanic eruptions in the Azores with brief reports. Boletim do Museu e Laboratório Mineralógico e Geológico da Faculdade de Ciências (10), 3–18.

Wohletz, K. H., Sheridan, M. F., 1983. Hydrovolcanic explosions; II, Evolution of basaltic tuff rings and tuff cones. American Journal of Science 283 (5), 385–413.

Zanon, V., 2015. Chapter 5 The magmatism of the Azores Islands. Geological Society, London, Memoirs 44 (1), 51–64.

Zanon, V., Pacheco, J., Pimentel, A., 2009. Growth and evolution of an emergent tuff cone: Considerations from structural geology, geomorphology and facies analysis of São Roque volcano, São Miguel (Azores). Journal of Volcanology and Geothermal Research 180 (2-4), 277–291.

Zhao, Z., Mitchell, N. C., Quartau, R., Tempera, F., Bricheno, L., 2019. Submarine platform development by erosion of a surtseyan cone at Capelinhos, Faial island, Azores. Earth Surface Processes and Landforms 0 (0).

CRediT author statement - VOLGEO_2019_397

Ricardo S. Ramalho:
Conceptualization; Investigation; Writing - Original Draft; Writing - Review & Editing; Visualization; Funding acquisition.

Rui Quartau:
Conceptualization; Investigation; Writing - Review & Editing; Visualization; Project administration; Funding acquisition.

Ármann Höskuldsson:
Investigation; Writing - Review & Editing.

José Madeira:
Investigation; Writing - Review & Editing; Funding acquisition.

João Ventura da Cruz:
Software; Formal analysis; Investigation; Visualization; Data Curation.

Aurora Rodrigues:
Investigation; Writing - Review & Editing; Project administration; Funding acquisition.

Declaration of interests

☒ The authors declare that they have no known competing financial interests or personal relationships that could have appeared to influence the work reported in this paper.

☐The authors declare the following financial interests/personal relationships which may be considered as potential competing interests:

Highlights

- High-resolution bathymetry reveals submerged young tuff ring at Santa Maria Island
- Morphology and correlation with relative sea level suggests ~43 ka of age
- Subaerial consolidation is key to preserve tuff rings from marine erosion
- Observations indicate volcanism at Santa Maria extended to late Pleistocene
- High-resolution bathymetry is key to volcanic hazard assessments of oceanic islands

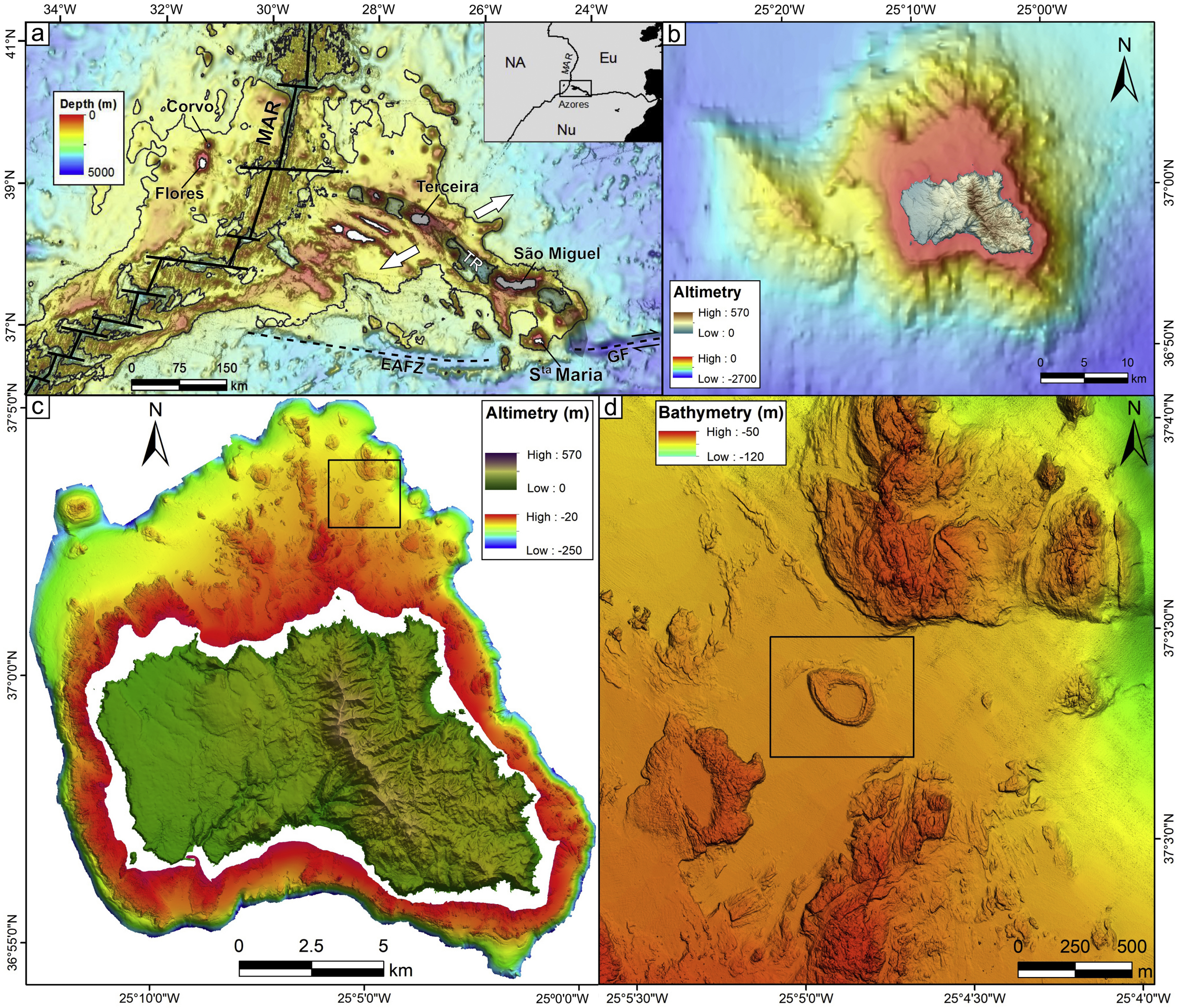
a
34°W
32°W
30°W
28°W
26°W
24°W
41°N
39°N
37°N
Depth (m)
0
5000
Corvo
Flores
MAR
Terceira
São Miguel
TR
EAFZ
GF
Sta Maria
0
75
150
km
NA
Eu
MAR
Azores
Nu
b
25°20'W
25°10'W
25°00'W
37°00'N
36°50'N
N
Altimetry
High : 570
Low : 0
High : 0
Low : -2700
0
5
10
km
c
37°5'0"N
37°0'0"N
36°55'0"N
25°10'0"W
25°5'0"W
25°0'0"W
N
Altimetry (m)
High : 570
Low : 0
High : -20
Low : -250
0
2.5
5
km
d
Bathymetry (m)
High : -50
Low : -120
N
37°4'0"N
37°3'30"N
37°3'0"N
25°5'30"W
25°5'0"W
25°4'30"W
25°4'0"W
0
250
500
m

Figure 1

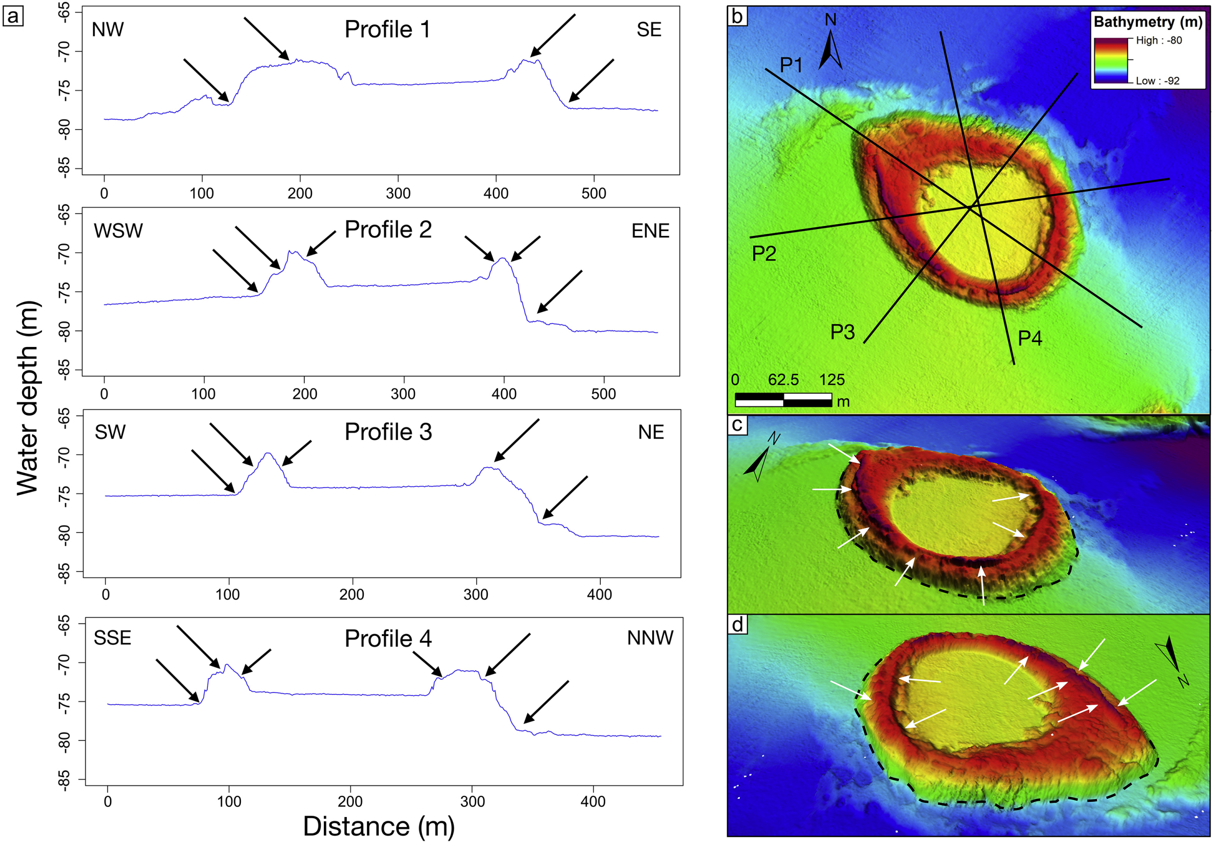
a
Water depth (m)
Distance (m)
Profile 1
NW
SE
Profile 2
WSW
ENE
Profile 3
SW
NE
Profile 4
SSE
NNW
-65
-70
-75
-80
-85
0
100
200
300
400
500
b
N
P1
P2
P3
P4
Bathymetry (m)
High : -80
Low : -92
0
62.5
125
m
c
N
d
N

Figure 2

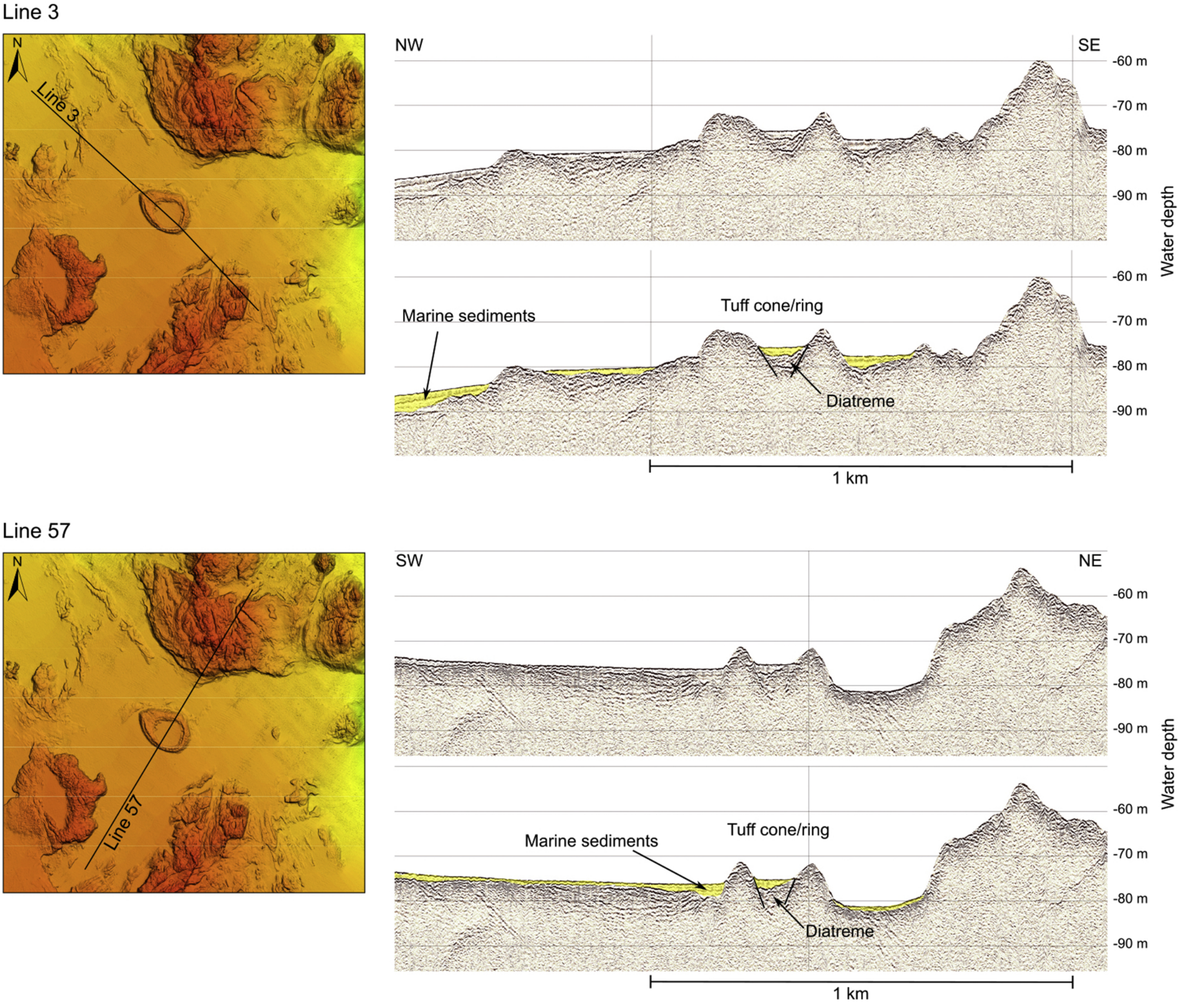
Line 3
N
Line 3
NW
SE
-60 m
-70 m
-80 m
-90 m
Water depth
Marine sediments
Tuff cone/ring
Diatreme
1 km
Line 57
N
Line 57
SW
NE
-60 m
-70 m
-80 m
-90 m
Water depth
Marine sediments
Tuff cone/ring
Diatreme
1 km

Figure 3

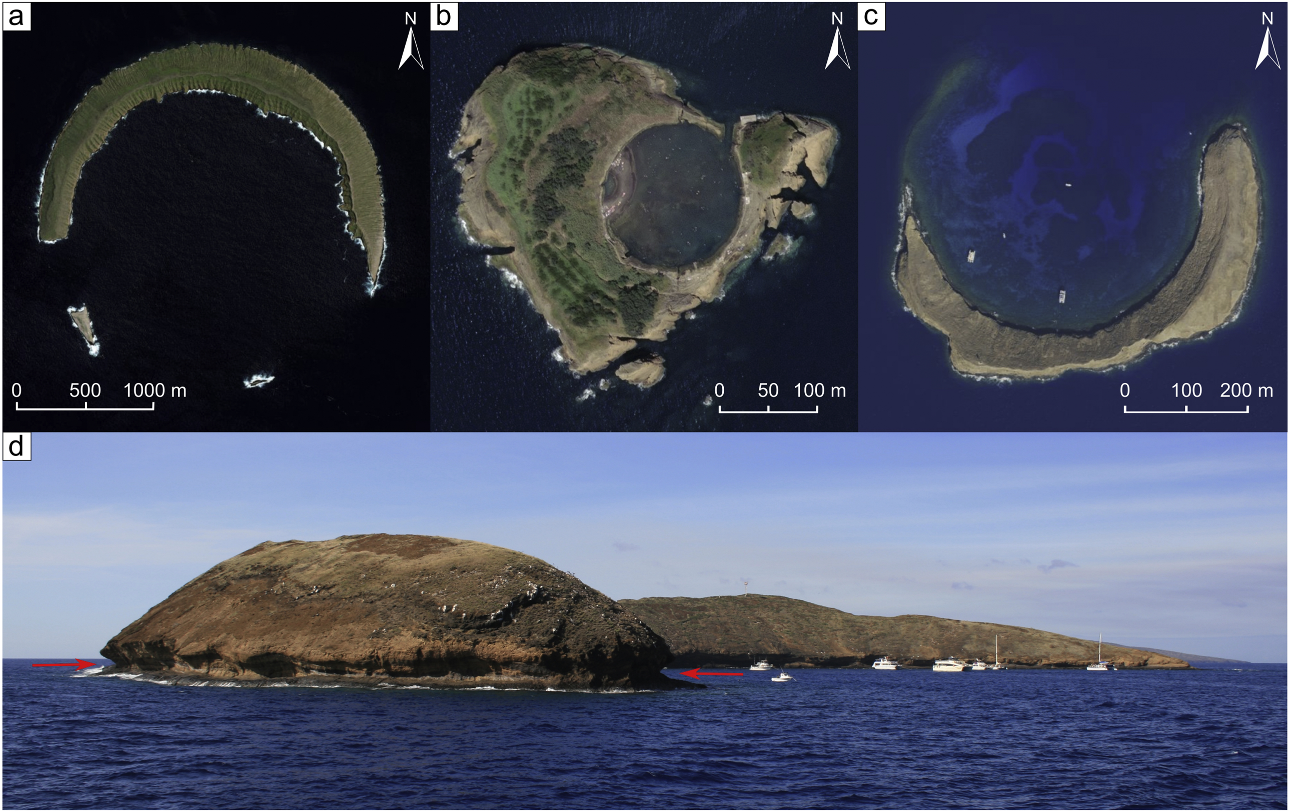

Figure 4

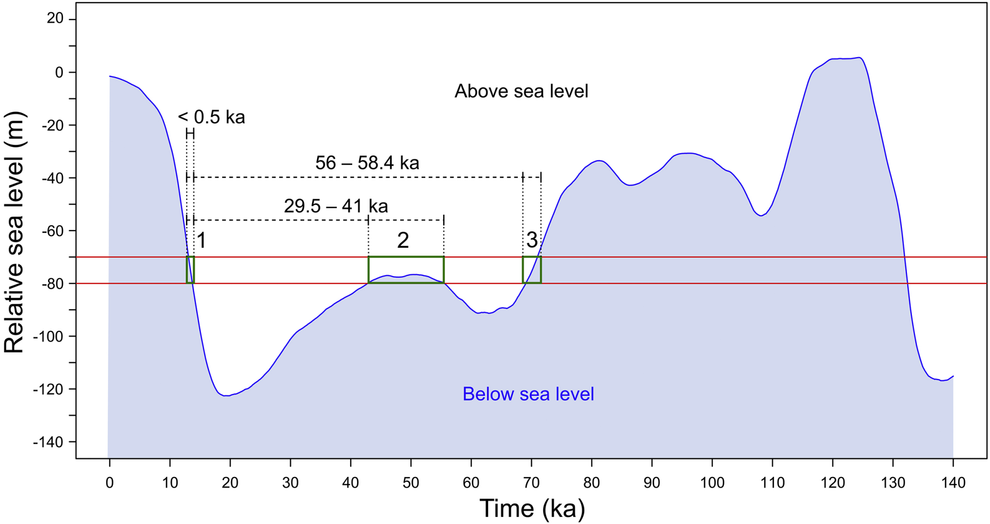
Relative sea level (m)
20
0
-20
-40
-60
-80
-100
-120
-140
Above sea level
Below sea level
< 0.5 ka
56 – 58.4 ka
29.5 – 41 ka
1
2
3
0
10
20
30
40
50
60
70
80
90
100
110
120
130
140
Time (ka)

Figure 5

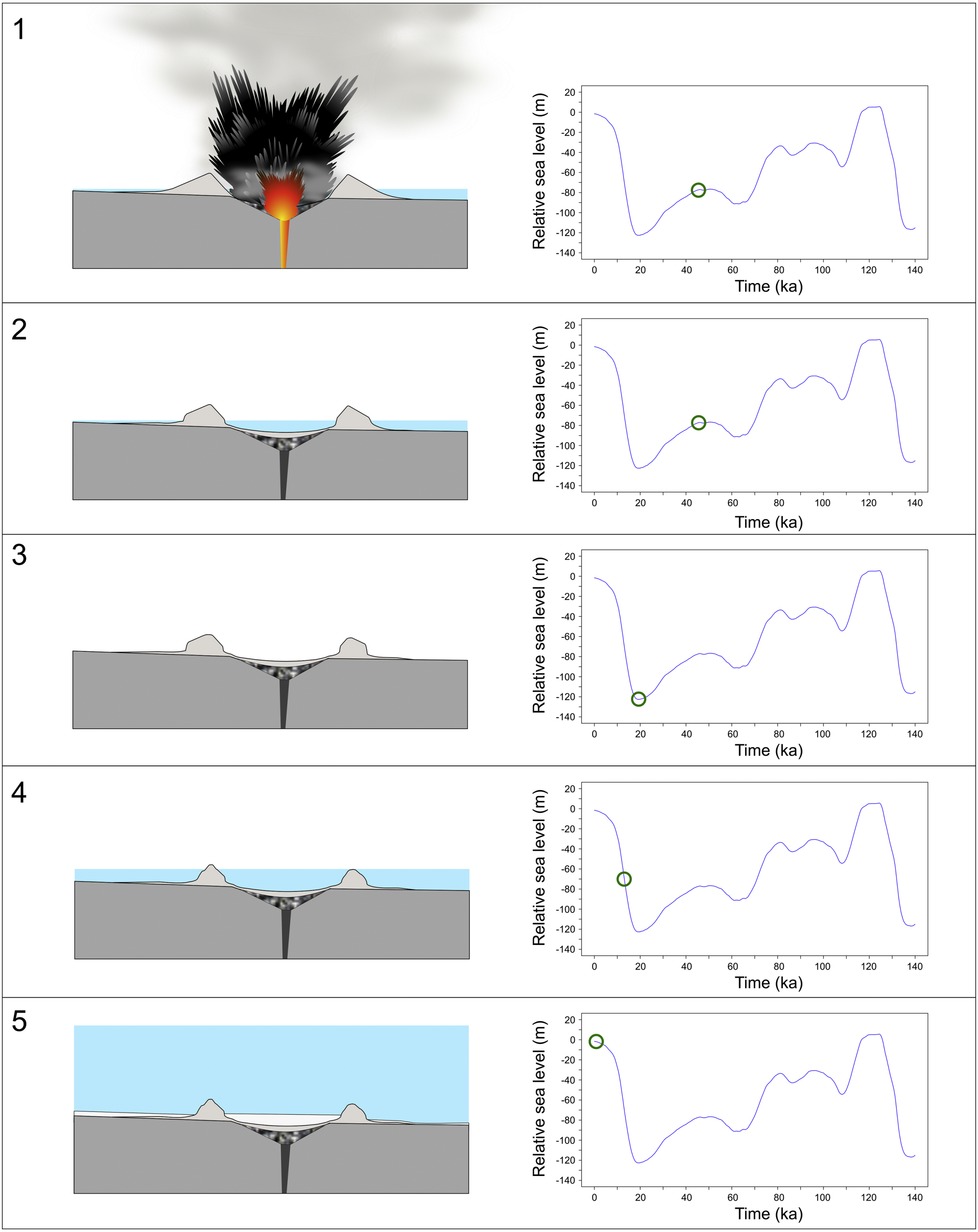
1
Relative sea level (m)
20
0
-20
-40
-60
-80
-100
-120
-140
0
20
40
60
80
100
120
140
Time (ka)
2
Relative sea level (m)
Time (ka)
3
Relative sea level (m)
Time (ka)
4
Relative sea level (m)
Time (ka)
5
Relative sea level (m)
Time (ka)

Figure 6